

Segment Anything Model for Zero-shot Single Particle Tracking in Liquid Phase Transmission Electron Microscopy

Risha Goel¹, Zain Shabeeb¹, Isabel Panicker¹, Vida Jamali^{1*}

¹School of Chemical and Biomolecular Engineering, Georgia Institute of Technology, Atlanta, Georgia, USA.

*Corresponding author(s). E-mail(s): vida@gatech.edu;

Contributing authors: rgoel63@gatech.edu; zshabeeb3@gatech.edu; ipanicker@gatech.edu;

Abstract

Liquid phase transmission electron microscopy (LPTEM) offers an unparalleled combination of spatial and temporal resolution, making it a promising tool for single particle tracking at the nanoscale. However, the absence of a standardized framework for identifying and tracking nanoparticles in noisy LPTEM videos has impeded progress in the field to develop this technique as a single particle tracking tool. To address this, we leveraged Segment Anything Model 2 (SAM 2), released by Meta, which is a foundation model developed for segmenting videos and images. Here, we demonstrate that SAM 2 can successfully segment LPTEM videos in a zero-shot manner and without requiring fine-tuning. Building on this capability, we introduce SAM4EM, a comprehensive framework that integrates promptable video segmentation with particle tracking and statistical analysis, providing an end-to-end LPTEM analysis framework for single particle tracking. SAM4EM achieves nearly 50-fold higher accuracy in segmenting and analyzing LPTEM videos compared to state-of-the-art methods, paving the way for broader applications of LPTEM in nanoscale imaging.

Main

Single particle tracking (SPT) is a method that tracks the motion of a particle over time as it interacts with its surroundings to infer and characterize the complex microscopic features of its surrounding environment [1, 2]. Several types of optical microscopy methods are currently used for SPT, the majority of which require inherently fluorescent or fluorescently labeled particles. In recent years, there have been efforts to develop a new microscopy modality, liquid phase transmission electron microscopy (LPTEM), as a label-free SPT method [3–6]. LPTEM introduces the ability to directly visualize nanoparticles with unprecedented spatiotemporal resolution (nanometer and millisecond) and with full rotational and conformational information in real-time. This visualization is realized using the accelerating electron beam of a transmission electron microscope (TEM) traveling through silicon nitride (SiN_x) membranes of a microfluidic chamber that hermetically seals the liquid sample. State-of-the-art in situ electron detectors enable users to acquire videos of nanoscale particles (as small as one nanometer [7]) at hundreds of frames per second (fps). The videos collected from LPTEM experiments can then be segmented and analyzed to track the diffusive motion of nanoscale probe particles over multiple decades in time (from 0.001 seconds to 100 seconds) to investigate the underlying physical rules governing their motion and interaction with their surroundings.

One of the significant challenges impeding progress in the field of LPTEM as an SPT method is that, unlike the optical microscopy field [8–10], there is no standardized end-to-end video processing framework that can segment the videos of moving particles, track them over time to arrive at spatiotemporal trajectories,

and analyze those obtained particle trajectories. The low signal-to-noise ratio (SNR) of noisy TEM images, which is exacerbated by the addition of the noise from the liquid layer in the LPTEM chamber, leaves current segmentation algorithms developed for optical microscopy inadequate for LPTEM video segmentation. Additionally, given the stochasticity in behaviors that are unique to the nanoscale, the nanoparticles may take large displacements between two consecutive frames, moving in and out of frame. Thus, it is incredibly important for the segmentation algorithm to provide a venue for receiving user prompts to identify the target particles to be tracked and distinguished from artifacts in the videos. Once a successful segmentation is achieved, the segmented masks must be linked together to form a trajectory of each tracked particle over time without losing the particles when they cross paths with each other. Thus, the algorithm must maintain a memory of the particles from previous frames to inform the rest of the tracking throughout the video to accommodate the tracking of multiple particles per video simultaneously.

Despite the pressing need from the community for a processing framework that addresses all these challenges, no comprehensive method exists. There have been efforts in recent years to address some of these challenges by developing deep learning models to segment static TEM images [11–15]. However, these models fail to generalize to new experimental data, particularly when liquid is present, thus requiring fine-tuning or retraining for each new dataset and lab setting (e.g., electron beam dose rate, magnification, etc). Additionally, the existing models are designed to treat each frame of the video independently [11, 14], losing the temporal context of the video that is critical to processing LPTEM videos and tracking multiple particles with complex motions. Thus, a transformative solution is needed—one that adapts seamlessly to new experimental conditions without retraining, remains robust to noise, is designed for video segmentation with a memory of past frames, and is continuously improved and updated, democratizing access to LPTEM as a SPT method for diverse users across different labs and disciplines.

The emergence of foundation models, i.e., large-scale artificial intelligence (AI) models trained on massive and diverse datasets, has been a game-changer in computer vision, enabling more accurate, adaptable, and scalable solutions for video segmentation tasks in several domains, from medical imaging [16] to autonomous vehicles [17]. Very recently, Meta released the Segment Anything Model 2 (SAM 2), which is the generalization of its predecessor, SAM [18], to the video domain. SAM 2 is a foundation model for promptable video segmentation with a vision-transformer architecture, trained on 50.9K videos and with 93.7 million parameters, outperforming established video segmentation benchmarks in the literature [19]. SAM 2 is capable of segmenting as well as identifying and isolating objects even when they move in and out of the frame and cross paths with each other, a feature critical to particle tracking. The key to the success of SAM 2 is in the architecture of the model, in which the prediction of the segmentation mask on a given frame is conditioned on the user prompt and/or on the memory bank of previously segmented frames [19].

In this work, we demonstrate the proof-of-concept performance of SAM 2 in achieving the video segmentation task in a zero-shot manner on noisy LPTEM videos without any need for retraining. Access to these segmented videos then unlocks the capability to use open-source Python-based libraries to extract the centroid positions and orientations of the masked particles in time. This allows for the statistical analysis of the obtained spatiotemporal trajectories of the particles in the video. Bringing these two modules together, we present SAM4EM, a unifying framework designed for SPT in LPTEM (Fig. 1). SAM4EM is designed with an interactive user interface to receive a user prompt to annotate which particles need to be tracked throughout the video by clicking on the target nanoparticles and/or providing a bounding box on each nanoparticle in a few frames of the video (Fig. 1b). Fig. 1a,c present the two modules used in SAM4EM. To showcase the power of SAM4EM on LPTEM data, we applied it on an LPTEM video acquired at an electron beam dose rate of $35 \text{ e}^-/\text{\AA}^2\cdot\text{s}$ and at a frame rate of 80 fps—equivalent to 0.0125 seconds exposure time—see Methods for experimental details. The first module takes in the frames of the LPTEM video, along with a user prompt (clicks on the particles, bounding boxes, or a combination of both), and outputs the segmented video as a binarized masked video (Fig. 1a). In this case, SAM 2 was prompted with one click on the first frame for each of the four particles visible in the video and successfully segmented the LPTEM video in a zero-shot manner, outputting a binarized video with four masklets—spatiotemporal masks (see video S1). The binarized video with indexed masklets is then the input for the second module, which locates the centroid position and orientation of each particle over time (Fig. 1c). The output of the second module is the spatiotemporal trajectories of the particles in a given LPTEM video, presented in different colors in Fig. 1c, together with relevant statistical analyses for each particle trajectory over time. Fig. 1d shows the corresponding time-averaged mean squared displacement (tMSD), the probability distribution of displacements, and the velocity autocorrelation for the trajectories shown in Fig. 1c.

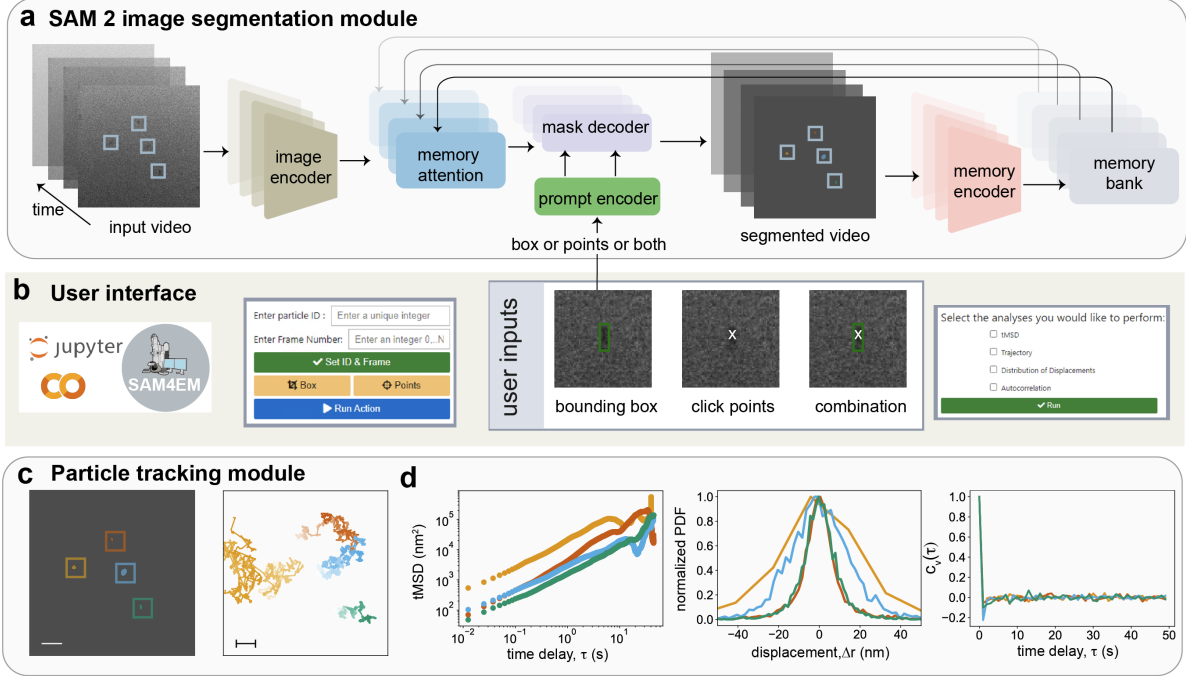


Fig. 1 SAM4EM for single-particle tracking in LPTEM. **a**, The architecture of the SAM 2 model used to segment an LPTEM video with four target nanoparticles, each annotated with a single point prompt on the first frame. **b**, The SAM4EM interactive interface is compatible with JupyterLab and Google Colab. Users interact with the selected video frames to identify the target particles via a bounding box and/or point prompts and then select the desired statistical tests to perform on the obtained particle trajectories. **c**, The trajectories of each target nanoparticle are extracted from the segmented video, and the selected statistical analyses are performed. From left to right: the spatiotemporal trajectories (with color intensity indicating increase in time from 0 to 45 seconds), time-averaged mean squared displacements, distribution of displacements, and velocity autocorrelation for each tracked nanoparticle (in different colors) in the LPTEM video. Scale bar, 250 nm.

To test the accuracy of the SAM4EM framework, we simulated synthetic single-particle LPTEM videos with ground truth masklets. The position of the particle in the simulated frames is derived from experimental trajectories collected from LPTEM experiments that do not necessarily follow a random Brownian motion [3]. The frames of the videos were simulated with noise functions relevant to LPTEM experiments as described in the literature, accounting for noise from electron beam-sample interaction, shot noise, and Gaussian white noise [11]. This enabled us to vary the sample thickness to simulate videos with a range of experimentally relevant SNR values. Therefore, these videos closely capture the behavior of experimental data while having well-defined ground truth masklets and centroid positions. Fig. 2a-c shows the first frames of three example videos simulated for LPTEM experiments with a gold nanorod diffusing in 5, 50, and 150-nanometer thick water layers encapsulated inside the liquid cell chamber with two SiN_x membranes, each of 50-nanometer thickness, along with the corresponding SNR values (Fig. 2d). The results of applying the SAM 2 module on these simulated videos were evaluated using the common $\mathcal{J}\&\mathcal{F}$ accuracy metric (the higher, the better) as a function of sample thickness. Fig. 2e shows the performance of the model using one click, a bounding box, or a combination of both to annotate the target nanoparticle on two frames of the video ($i = \{1, 125\}$) as a user prompt. The results demonstrate that SAM4EM successfully segments the videos with a $\mathcal{J}\&\mathcal{F}$ score of $\geq 70\%$. We compare our approach with a U-Net model, a deep learning architecture widely used for image segmentation, which was trained on LPTEM images [11], with an average $\mathcal{J}\&\mathcal{F}$ score of $\leq 2\%$ in zero-shot segmentation task. As shown in Fig. 2d, this comparison highlights the superior performance of SAM4EM in processing LPTEM videos compared to state-of-the-art methods in LPTEM literature.

This study showcases the enormous potential of vision foundation models for microscopy data processing and, in particular, the SPT research field. The exceptional performance of the SAM 2 module on zero-shot segmentation of noisy LPTEM videos highlights the remarkable power of large-scale AI models to generalize

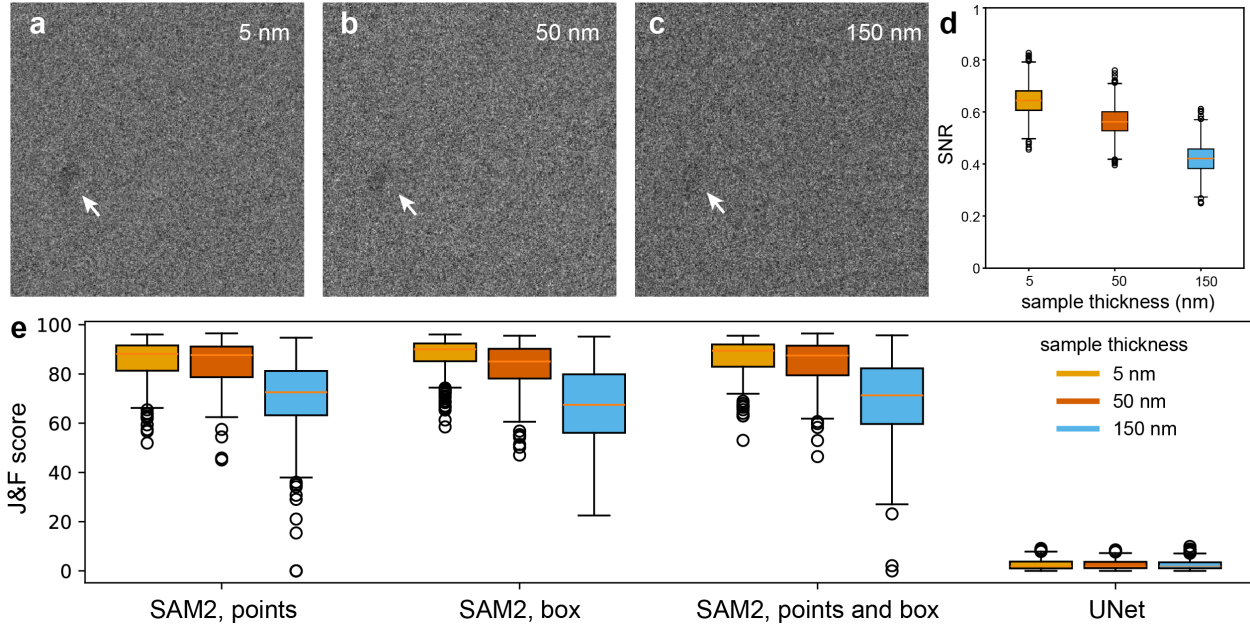


Fig. 2 Zero-shot accuracy in segmentation on simulated datasets. **a-c**, The first frame of LPTEM videos simulated with a sample thickness of (a) 5 nm, (b) 50 nm, and (c) 150 nm. The white cursor indicates the nanoparticle. **d**, Box plots showing the distribution of the signal-to-noise ratio (SNR) across the 275 frames of the simulated LPTEM video at each sample thickness. The box spans the 1st to the 3rd quartile of the SNR data. The orange line indicates the median SNR. Whiskers extend to $1.5\times$ the interquartile range, and circles denote outliers beyond this range. **e**, Box plots of the per-frame $\mathcal{J}\&\mathcal{F}$ score, demonstrating the performance of various segmentation methods on the 275 frames of the simulated video for each sample thickness in (a-c). From left to right: SAM 2 using a point annotation on two frames, SAM 2 using a bounding box annotation on two frames, SAM 2 using a point and a box annotation on two frames, in comparison to the baseline U-Net model [11].

to new datasets. The democratization of processing software that benefits from continuous improvements and updates, such as SAM 2, standardizes data processing across research labs and promotes scientific reproducibility. The latter is significantly crucial for a new research field such as LPTEM. We anticipate that other features of this framework, including the real-time segmentation at the speed of close to 50 fps, will be advantageous for the microscopy field once integrated with the microscope control software, advancing the field of AI-in-the-loop for microscopy towards automatization of microscopes [20, 21].

Methods

LPTEM experiment

Microfabricated silicon nitride chips from Protichips Inc. were used to encapsulate the gold nanorod solution for LPTEM imaging. The bottom chip (Protochips ID EPB-55-BNS10) has a silicon nitride window with dimensions $550\ \mu\text{m}$ by $50\ \mu\text{m}$ with a 50 nm static spacer. The top chip has (Protochips ID EPT-55W-10) has silicon nitride window with dimensions $550\ \mu\text{m}$ by $50\ \mu\text{m}$. The chips were cleaned by sequential immersion in acetone and ethanol baths, followed by drying with nitrogen gas blown parallel to the surface. To ensure uniform spreading of the liquid solution across the chip surface, the chips were treated with a glow discharge using a PELCO easiGlow system at 0.39 mBar pressure for 45 seconds. After cleaning, the chips were assembled into a liquid cell using the Poseidon Select holder from Protochips Inc. A volume of $0.5\ \mu\text{L}$ of gold nanorod solution was placed between the two chips. The assembled liquid was hermetically sealed to prevent evaporation into the TEM.

Aqueous dispersion of gold nanorods ($60\ \text{nm} \times 40\ \text{nm}$ with cetyltrimethylammonium chloride (CTAC) ligands) was encapsulated in the liquid cell. The assembled liquid cells were imaged on an FEI Tecnai F30 TEM at 200 kV with a Gatan OneView in situ camera. Videos were recorded at an electron beam dose rate of $35\ \text{e}^-/\text{\AA}^2\text{-s}$, a magnification of 19.5 kx, and a resolution of 1024×1024 pixels at 80 frames per second. Experimental LPTEM data was captured with a resolution of 1024-by-1024 pixels at a rate of 80 frames per second.

LPTEM data pre-processing

In-situ LPTEM data was collected in .dm4 format directly using Digital Micrograph software on a Gatan Oneview in situ camera. For multiple particle tracking purposes, each frame of the acquisition is directly exported to a .tiff file from Digital Micrograph, without the need to crop the field of view to a single particle. An in-house Python algorithm converts the .tiff files to 8-bit, 3-channel RGB JPEG files and subsequently renames the files to frame_<frame_index>.jpeg, where <frame_index> is the frame number padded with zeros to be 6 digits long, compatible with SAM 2.

LPTEM simulated videos

LPTEM simulated videos were generated using the method described previously by Yao et al. [11]. The original MATLAB code was converted to Python and modified for the experimental conditions described here (e.g., water thickness, particle shape and size, and electron beam dose rate).

SAM 2 video segmentation

The original SAM 2 video segmentation model, published by Meta, was adapted to create a more intuitive user interface for particle segmentation tracking. Interactive Jupyter notebook controls were integrated to replace the manual input of bounding box coordinates or points prompts and their labels directly in the code. The modifications enable the user to select the Particle ID of their particle of interest and their desired input prompt type and then directly interact with their selected frame by clicking to mark prompts. Once achieving the desired result on the first frame, the user can choose to propagate the segmentation throughout the video.

Single particle trajectory analysis

The centroid (x, y) and orientation (in-plane angle, θ) of each particle in each frame are calculated from the segmented mask array in the Particle Tracking module. The data is saved as a .csv file.

To characterize the diffusive behavior of nanoparticles in LPTEM experiments, we analyzed the trajectories using three key statistical metrics presented in Figure 1d.

Time-averaged Mean Squared Displacement

The tMSD(τ) quantifies the average displacement of a particle over time delay, τ . It is given by:

$$\text{tMSD}(\tau) = \langle (\mathbf{r}(t + \tau) - \mathbf{r}(t))^2 \rangle, \quad (1)$$

where $\mathbf{r}(t)$ and $\mathbf{r}(t + \tau)$ represent the particle's positions at time t and $t + \tau$, respectively. $\langle \cdot \rangle$ denotes the mean value over frames of a single trajectory.

Velocity Autocorrelation

The velocity autocorrelation function, $C_{\mathbf{v}}(\tau)$, measures the temporal memory of a particle's motion and is defined as:

$$C_{\mathbf{v}}(\tau) = \frac{\langle \mathbf{v}(t) \cdot \mathbf{v}(t + \tau) \rangle}{\langle \mathbf{v}(t)^2 \rangle}, \quad (2)$$

where $\mathbf{v}(t)$ and $\mathbf{v}(t + \tau)$ represent the particle's velocities at time t and $t + \tau$, respectively. This function indicates whether the motion is correlated, uncorrelated, or anti-correlated.

Distribution of Displacements

The distribution of displacements provides statistical information about the nature of the particle's motion. This is characterized by the probability density function (PDF) of particle displacements $\Delta \mathbf{r}$ over a fixed time interval. For Brownian motion, the distribution is Gaussian, while non-Gaussian processes may exhibit heavy tails or other deviations, reflecting the underlying physical mechanisms influencing the motion.

\mathcal{J} & \mathcal{F} accuracy metric

The accuracy of the segmentation on the simulated single-particle datasets was evaluated using the \mathcal{J} & \mathcal{F} metric [19] on a scale from 0% to 100%, where a score of 100% indicates that the prediction completely matches the ground truth.

The Jaccard Index \mathcal{J} assesses region similarity by calculating the intersection-over-union between the segmented mask (M) and the ground-truth (G): $\mathcal{J} = \frac{|M \cap G|}{|M \cup G|}$. The F-measure \mathcal{F} assesses the accuracy of the mask contour. \mathcal{F} is calculated from the contour-based precision (P_c) and recall (R_c) between the boundary pixels of the segmented mask and the ground-truth: $\mathcal{F} = \frac{2 * P_c * R_c}{P_c + R_c}$. See [22] for further details on the \mathcal{J} and \mathcal{F} metrics.

The \mathcal{J} & \mathcal{F} score of a frame is the average of the \mathcal{J} and \mathcal{F} of the frame [23]. The average \mathcal{J} & \mathcal{F} across the video is computed using the per-frame scores.

U-Net LPTEM image segmentation baseline

As a baseline, the U-Net model from Yao et al. [11] was used to segment the simulated datasets. The model was trained using the dataset provided by the authors for 20 epochs and with a learning rate of 1×10^{-6} .

Code Availability

All codes are available on Github, <https://github.com/JamaliLab/SAM4EM>.

Acknowledgments

This research was supported by the NSF, Division of Chemical, Bioengineering, Environmental, and Transport Systems under award 2338466, Georgia Tech Institute for Matter and Systems, Exponential Electronics seed grant, the American Chemical Society Petroleum Research Fund under award 67239-DNI5, and the Exponential Electronics Seed grant of the Institute for Matter and Systems at Georgia Tech. We acknowledge the support of the Material Characterization Facility and the Electron Microscopy Facility of the Institute for Matter and Systems at Georgia Tech.

Corresponding Author

Correspondence should be addressed to vida@gatech.edu.

Competing Interests

The authors declare no competing interests.

References

- [1] Simon, F., Weiss, L. E. & van Teeffelen, S. A guide to single-particle tracking. *Nature Reviews Methods Primers* **4**, 66 (2024).
- [2] Manzo, C. & Garcia-Parajo, M. F. A review of progress in single particle tracking: from methods to biophysical insights. *Reports on progress in physics* **78**, 124601 (2015).
- [3] Jamali, V. *et al.* Anomalous nanoparticle surface diffusion in lctem is revealed by deep learning-assisted analysis. *Proceedings of the National Academy of Sciences* **118**, e2017616118 (2021).
- [4] Chee, S. W., Anand, U., Bisht, G., Tan, S. F. & Mirsaidov, U. Direct observations of the rotation and translation of anisotropic nanoparticles adsorbed at a liquid–solid interface. *Nano letters* **19**, 2871–2878 (2019).
- [5] Wang, H., Xu, Z., Mao, S. & Granick, S. Experimental guidelines to image transient single-molecule events using graphene liquid cell electron microscopy. *ACS nano* **16**, 18526–18537 (2022).
- [6] Liu, S. *et al.* Observing ion diffusion and reciprocating hopping motion in water. *Science Advances* **9**, eadf8436 (2023).
- [7] Kang, S. *et al.* Real-space imaging of nanoparticle transport and interaction dynamics by graphene liquid cell tem. *Science Advances* **7**, eabi5419 (2021).
- [8] Crocker, J. C. & Grier, D. G. Methods of digital video microscopy for colloidal studies. *Journal of colloid and interface science* **179**, 298–310 (1996).
- [9] von Chamier, L. *et al.* Democratising deep learning for microscopy with zerocostdl4mic. *Nature communications* **12**, 2276 (2021).
- [10] Ershov, D. *et al.* TrackMate 7: integrating state-of-the-art segmentation algorithms into tracking pipelines. *Nature methods* **19**, 829–832 (2022).
- [11] Yao, L., Ou, Z., Luo, B., Xu, C. & Chen, Q. Machine learning to reveal nanoparticle dynamics from liquid-phase tem videos. *ACS central science* **6**, 1421–1430 (2020).
- [12] Kalinin, S. V. *et al.* Machine learning in scanning transmission electron microscopy. *Nature Reviews Methods Primers* **2**, 11 (2022).
- [13] Wang, X. *et al.* Autodetect-mnp: an unsupervised machine learning algorithm for automated analysis of transmission electron microscope images of metal nanoparticles. *JACS Au* **1**, 316–327 (2021).
- [14] Cheng, B., Ye, E., Sun, H. & Wang, H. Deep learning-assisted analysis of single molecule dynamics from liquid-phase electron microscopy. *Chemical Communications* **59**, 1701–1704 (2023).
- [15] Rangel DaCosta, L., Sytwu, K., Groschner, C. & Scott, M. A robust synthetic data generation framework for machine learning in high-resolution transmission electron microscopy (HRTEM). *npj Computational Materials* **10**, 165 (2024).
- [16] Zhao, T. *et al.* A foundation model for joint segmentation, detection and recognition of biomedical objects across nine modalities. *Nature Methods* 1–11 (2024).
- [17] Gao, H. *et al.* A survey for foundation models in autonomous driving. *arXiv preprint arXiv:2402.01105* (2024).
- [18] Kirillov, A. *et al.* Segment anything. *Proceedings of the IEEE/CVF International Conference on Computer Vision* 4015–4026 (2023).

- [19] Ravi, N. *et al.* SAM 2: Segment anything in images and videos. *arXiv preprint arXiv:2408.00714* (2024).
- [20] Spurgeon, S. R. *et al.* Towards data-driven next-generation transmission electron microscopy. *Nature materials* **20**, 274–279 (2021).
- [21] Kalinin, S. V. *et al.* Machine learning for automated experimentation in scanning transmission electron microscopy. *npj Computational Materials* **9**, 227 (2023).
- [22] Perazzi, F., Khoreva, A., Benenson, R., Schiele, B. & Sorkine-Hornung, A. Learning video object segmentation from static images. *Proceedings of the IEEE conference on computer vision and pattern recognition* 2663–2672 (2017).
- [23] Pont-Tuset, J. *et al.* The 2017 davis challenge on video object segmentation. *arXiv preprint arXiv:1704.00675* (2017).